An Observational Study of the Summer Mediterranean Sea-Breeze-Front Penetration into the Complex Topography of the Jordan-Rift-Valley

By:

R. Naor[1], O. Potchter[2], H. Shafir[3] and P. Alpert[3]

[1]The Porter School of the Environmental Studies, Tel Aviv University, Tel Aviv, Israel, 69978

[2]Dept. of Geography and Human Environment, Tel Aviv University, Tel Aviv, Israel, 69978

[3]Dept. of Geosciences, Tel Aviv University, Tel Aviv, Israel, 69978

Submitted to: Theoretical and Applied Climatology-Revised

July 2015

Corresponding Author: Pinhas Alpert, Dept. of Geosciences, Tel Aviv University, Tel Aviv, Israel, 69978, e-mail: pinhas@post.tau.ac.il, Tel. 972-3-6407380, fax: 972-3-6409282

ABSTRACT

The Mediterranean summer sea breeze front (SBF) climatic features of penetration into the complex topography of the Jordan Rift Valley (JRV) were investigated. It was shown that the SBF penetration into the JRV occurs in a well-defined chronological order from north to south. One exception to this general rule is the breeze penetration of Sdom, which occurs after it has penetrated the Arava which is located further south, probably due to the micro-climatic effect of the Dead-Sea. It was also noted that the breeze increases the local specific humidity as it reaches the JRV in spite of significant temperature increases. The temperature reaches its daily peak two to three hours later in the southern valley compared to the northern valley, and is suggested to be due to the later SBF penetration and the valley structure. The pre-SBF lines features in the JRV are described.

KEY WORDS: Jordan Rift Valley, Mediterranean Sea Breeze, Dead Sea Lake Breeze, Sea Breeze Front, Pre Sea Breeze Front

1. Introduction

The Jordan Rift Valley (JRV), also known as ‘The Jordan-Dead Sea Rift’, is a valley dividing Israel to the west from the Kingdom of Jordan and Syria to the east. Its distance from the Mediterranean Sea varies from approximately 40 km in the north to as much as 110 km in the south (Fig. 1, Tab. 1).

The sea breeze is caused by the response to the daytime differential heating between land and sea which creates a horizontal pressure gradient thus enabling cool and humid marine air to penetrate inland. The sea breeze is also influenced by the strength and direction of the synoptic scale wind patterns, atmospheric stability and local topography features. Over sub-tropical regions like that of the East Mediterranean (EM), these phenomena are most pronounced during the summer season when the land-sea temperature differences are the largest (extensive reviews can be found in e.g., Simpson, 1994; Crosman and Horel, 2010).

The sea breeze along the EM coast and the inland and its relationship with the Etesian winds in the summer season, as well as with the topography were studied and simulated in early numerical mesoscale studies (Doron & Neumann, 1977; Alpert et al., 1982; Segal et al., 1983; Mahrer, 1985; Segal et al., 1985; Goldreich et al., 1986; Alpert & Getenio, 1988; Feliks, 2004; Saaroni et al., 2004; Lensky and Dayan, 2012),

The strong winds (of about 10 m/s) associated with the Mediterranean Sea breeze (MSB) are considered one of the most significant meteorological phenomena of the summer season in the JRV. At this time of year, the weather in this region is fairly stable, especially in July and August, due to the dominance of the subtropical high and the Persian Trough over the region (Skibin and Hod, 1979; Alpert et al., 1990; Bitan and Saaroni, 1992; Saaroni and Ziv, 2000). These synoptic conditions allow the MSB to develop in the morning along the coast of the Mediterranean Sea, then to penetrate inland, superimposed with the Etesian winds (the wind resulting from the prevailing synoptic system), and to reach the JRV in the afternoon, where it remains dominant for several hours (Bitan 1974, 1977). On the Mediterranean coast, the MSB is westerly and it veers clockwise to the north by the time it arrives to the JRV due to both the Coriolis force and the channelling effect, which is created by the topographical structure of the JRV area (Alpert & Getenio, 1988; Saaroni et al. 2004). In the Dead Sea area, the dominant MSB wind direction is north-westerly.

Lensky and Dayan (2012) detect and characterize the MSB progress under clear sky conditions during the summer, using remote sensing data and concurrent field measurements. They found that over desert regions the strong thermal contrast enables the detection of the MSB under synoptic conditions characterized by strong horizontal pressure gradient such as the deep Persian Trough.

Previous studies of the Dead Sea climate have demonstrated that, when the MSB descends about 1200 m from the mountains to the valley, it speeds up and the adiabatic heating warms the Dead Sea area (Ashbel, 1939; Alpert et al., 1997; Shafir and Alpert, 2011). Other studies examined the effect of the MSB while focusing on the local climate in small scale areas in the JRV: the Sea of Galilee

(Alpert et al., 1982), and the Sea of Galilee as compared to the Dead Sea (Bitan, 1982), Eilat in the southern part of the Arava Valley (Saaroni et al., 2004).

The purpose here is to investigate the MSB penetration into the JRV during summer, focusing on the exact times that the MSB reaches several stations in the JRV by analyzing real data from six locations along the JRV from north to south: the Hula Valley, the Sea of Galilee, the Central Jordan Valley, the Dead Sea and the northern part of the Arava Valley. This study investigates the features of the MSB as it penetrates into the JRV.

2. Methodology

2.1 Study area

The Jordan Rift Valley (JRV) extends for 420 kilometers from north to south, stretching from the Hula Valley to the Red Sea (Fig. 1). The JRV is a narrow, elongated valley, situated in the northern section of the East African Rift that extends from the Taurus Mountains in Turkey to East Africa. It is divided into four major sections, as follows: 1) the northern area extends from the Lebanese-Syrian border, about 100 m above MSL, to the southernmost point of the Sea of Galilee located about 210 m below MSL. 2) The central area, a valley about 100 km long and 4-16 km wide, between the Sea of Galilee and the Dead Sea. 3) The Dead Sea area, the lowest point on Earth (430 m below MSL). 4) The Arava, stretching north-south from the Dead Sea to the Red Sea coast and the city of Eilat. The JRV runs approximately parallel to the Mediterranean coast, from which it is separated by 40-110 km of coastal plain and inland hills, rising to a maximum height of 1200 m and an average height of 800 m (Cohen and Stanhill, 1996). The differences in height between the Judean Mountains and the Dead Sea Valley vary from 1200 m to 1400 m, sometimes over an aerial distance of only 23 km (Bitan, 1977). This unique complex topography is of special interest for the JRV studies including the current one.

2.2 Meteorological background and data

The JRV stretches along three quite different climatic zones: Mediterranean in the north, semi-arid in the center, and hyper-arid in the south.

The main factors influencing the climate of the JRV are the topographical height differences, the shape of the local complex topography, the subsiding winds from the Judean and Samarian hills, and the development of local breezes (Bitan, 1982,; Alpert et al., 1997). Alpert and Eppel (1985) suggested an index for mesoscale activity (I). When this index is higher than 1 the mesoscale winds are governing over the large-scale winds, and the opposite when I is lower than 1. They have shown that the JRV is dominated by very high mesoscale activity particularly in the summer[1] (I~2-4), demonstrating that the JRV circulations are most dominant when compared to the large-scale wind component in the JRV.

Here, meteorological data was taken from six official weather stations operated by the Israeli Meteorological Service, representing sub-areas along the JRV (Fig 1, Tab. 1): (1) Kfar Blum, the northernmost station, located in the Hula Valley (+75m), (2) Beit Tzaida, positioned 1.5 km eastern to the Sea of Galilee (-200m) — both stations are located in a Mediterranean climate. (3) Gilgal, 25 km

[1] The JRV is unique in acquiring high mesoscale activity even during winter ($I \geq 1$).

north of the Dead Sea in a semi-arid climate. (-255m) (4) Beit Haarava, on the northwestern edge of the Dead Sea, (-330m) (5) Sdom, located on a dike between the evaporation ponds at the southern edge of the Dead Sea (-388m), and last station (6) Hatzeva, situated 25 km south of the Dead Sea (-135m). Stations (4)-(6) are located in the hyper-arid climate (Fig 1).

2.3 Season and period of study

This study focuses on the mid-summer months, July and August, when the MSB is fairly consistent and has the highest average velocity. During July-August the weather is quite stable and the MSB blows almost every day, assisted by the synoptic winds which are also quite stable. Data from the period of July-August during the years 2008-2009 was collected and analysed here.

2.4 Data analysis

In order to demonstrate how the MSB penetrates the JRV, the following two methods were employed. First, data about wind speed and direction were 10-minutes averaged at the six aforementioned stations on a daily basis during July-August 2008-2009.

Second, turbulence intensity or gustiness analyses were performed following Alpert and Rabinovich-Hadar (2003). This variable emphasizes quick and drastic changes in wind speed over a short duration, such as occurs in a period of a few minutes. For this reason, it was shown as a good measure of the sea breeze fronts (SBF) penetration at the coastal plain (Alpert and Rabinovich-Hadar, 2003). Hence, this method was also employed here as a sensitive indicator for the

MSB penetration into the JRV. The gustiness is defined as the ratio between the wind speed standard deviation, $\sigma = \sqrt{\overline{v'^2}}$ and the average wind speed, $\bar{v}$ for 50 min time intervals, where v' is the wind speed taken as the 10 minute basic measurement (Alpert and Rabinovich-Hadar, 2003).

$$G = \frac{\sqrt{\overline{v'^2}}}{\bar{v}} = \frac{\sigma}{\bar{v}'}$$

In this study, averages were calculated for July-August during 2008-2009 (a total of 124 days), based on meteorological measurements with 10-min time interval.

Another measure for the MSB penetration into the valley is based upon the wind speed difference (Alpert and Rabinovich-Hadar, 2003). It consists of observing each wind speed data for 10 minutes and subtracting it from the measurement taken 20 minutes before, thus discovering rapid changes in wind speed.

Finally, running averages were calculated for wind speed, specific humidity and temperature based on the same time period.

3. Results and Discussion

3.1 Wind speed and gustiness of the Mediterranean Sea breeze

The MSB was observed in all stations every day during the study period. Fig. 2 shows the Jul-Aug average diurnal wind speed for the years 2008-2009. The maximum wind speed span was observed from 14:00 to 19:20 from north to south. That peak was identified in earliest studies as the MSB (Ashbel, 1939;

Bitan, 1974; Alpert et al, 1982). Fig. 3 and 4 present the identification of the time of the breeze penetration into the JRV based on the gustiness and wind speed difference (as explained in the previous section), while the peak in every station illustrates the Sea breeze front (SBF) penetration in both graphs. The examination of turbulence intensity or gustiness peak in the graph (Fig 3) shows that the daily appearance of the SBF varies from north to south, and that, as expected, the first gustiness peak occurs in the northern-most station, Kfar Blum, even before mid-day (~ 11:50 h). The next stations to reach the peak are Beit Tzaida, Gilgal and Beit Haarava, respectively. However, the peak in Hatzeva (the 6th station) appears before Sdom (the 5th station), which is located 30 km north of Hatzeva. This also happens in the wind speed difference graph (Fig 4). The reason for this chronological order of the MSB penetration from the Northern JRV to South is the combination of the distance of the observational point from the Mediterranean Sea and the mountain height west to the point (as clearly seen in Tab. 1) which increase from North to South, and limit the MSB. The probable cause of the delay in breeze penetration to Hatzeva before Sdom is the micro-climate of the Dead Sea. The micro-climate is affected by the easterly Dead Sea breeze on the west shores of the sea and the ponds and from the anabatic winds rising up the mountains surrounding the Dead Sea Valley which oppose the north and north-westerly MSB winds. These opposing winds delay the penetration of the MSB to the southern Dead Sea (Alpert et al., 1982, 1997, Shafir and Alpert, 2011). Shafir et al, (2011) pointed out that the Mediterranean Sea breeze, which reaches South Israel in the early evening hours, has recently become stronger due to the decreasing lake breeze effect. From a topo-climatic perspective, Hatzeva is located 270 m higher than Sdom, and has no tall mountains to its west (Tab. 1).

Due to this fact, the anabatic winds in this area are not significant, and therefore do not cause the additional delay. Also, in Hatzeva the Dead Sea breeze is very weak and blows from the north, thus not delaying the MSB. Bitan (1982) has noted that the MSB arrives to the southern parts of the Dead Sea half an hour later then to the north. This phenomenon can also be seen nowadays, as shown in figs 2, 3, and 4, in the MSB penetration time gap between Beit Haarava and Sdom. In summary, this delay seems to result from two main factors: 1) Geographic location - the Sdom station is located 85 km south of Beit Haarava, at a larger distance from the Mediterranean Sea coast. 2) The topography to the west of the stations - high cliffs rise to the west of Beit Haarava. The cliffs speed up the MSB that descends from the northwest and assist it against the opposing of both the anabatic winds and the Dead Sea breeze. This effect was also suggested by Alpert et al. (1982) at the Sea of Galilee. The cliffs that lie to the west of the Hatzeva station, however, are not as high and are located further away than the ones in the Sdom area, thus they have a reduced effect on the MSB.

It can be concluded that the MSB arrives to the stations in the JRV during the summer from north to south order until it reaches the Dead Sea. This is because of the distance from the Mediterranean Sea and the mountain heights west to the measuring point. The micro-climate of the Dead Sea delays the penetration of the MSB to the area, and therefore modifies the north to south order of arrival.

Additional findings about the MSB arrival (Fig. 2) are:

1) The order of SBF arrival according to the peak in wind speed is the same as in the gustiness, a fact that reinforces our previous conclusions.

2) In all stations the wind speed peaks during the MSB arrival about 1.5-2 hours after the gustiness-based beginning of the MSB.

3) The MSB speed peaks at the stations around the Dead Sea and Lake Kinneret are about 7 m/s as a result of the descending wind from the Galilee, Samaria, Judea and the Negev mountains to the valley. In Kfar Blum, however, the peak is much lower (3.5 m/s), probably due to the height differences between the mountains and the station which are less significant.

4) The sharp increases in the wind speeds in all stations indicate the strength of the MSB penetration to the valley. After reaching its maximum speed, the MSB continues to blow intensely for a few minutes, and calms down gradually. Rapid changes in the breeze speed are also seen in the gustiness (Fig 3). The MSB high peaks are followed by rapid falls.

3.2 The effect of MSB penetration on humidity in the JRV

Fig. 5 shows the daily mean specific humidity changes in the JRV stations. As expected, the humidity increases coincide with the MSB penetration to the valley (Fig. 2-4). It is interesting to note that, even after more than 100 km of blowing over land, the wind (which originated in the Mediterranean Sea) still contains high humidity, and increases the humidity of the JRV while penetrating and afterwards. This happens even in Hatzeva 120 km away from the Meditteranean Sea coast (Fig.1, Tab. 1), and in spite of the temperature increase (see next section). In general, the humidity values decreased from north to south; this can be explained by the general character of the climate of Israel, and by the closer proximity of the more northern stations to the Mediterranean Sea. The earlier humidity increases in Sdom and Hatzeva are probably due to the earlier Dead-Sea breeze effect, This breeze effect cannot be observed at Bet Haarava since the station is located 3 km away from the lake and 130 meters above. Therefore, the humidity rise in this station is the last in order during the day as compared to the Sdom station, which is located near to the lake (Alpert et al., 1997; Shafir and Alpert 2011)..

3.3 The MSB penetration effect on the temperature in the JRV

Fig. 6 shows the temperature running mean in the JRV stations. There is a time interval delay of about 3h between the temperature peaks at the southern stations in respect to the Northern ones and the times of the temperature peaks appear at the same order as that of the wind peaks and gustiness (Figs. 2-4). There is one exception which is the later peak in Beit-Haarava, reached 20-40 minutes after the southern stations (Sdom and Hatzeva). These might be the outcome of the following:

1. The topographical structure of the valley plays an important role in determining the peak temperature. In the north the JRV structure is nearly flat and low, and therefore, the maximum temperature occurs around noontime. In the south, the narrow and deep JRV structure traps the warm air in the valley, and it cannot be affectively released before sunset. The exception of Beit Haarava is due to the aforementioned deeper and narrower structure of the valley in this area (Bitan, 1977, see Fig.6 for quantitative measures of this effect, see also Tab.1 here which shows that Beit Haarava is the deepest in the JRV among all the stations). This causes

the Beit Haarava peak temperature, and afterward the Sdom temperature to be the latest in comparison to Hatzeva and the Northern stations.

2. The MSB penetration in later hours in the south. While falling from the western mountain it warms adiabatically and increases the valley temperature in the afternoon, causing later peaks in the southern stations of the JRV (Bitan, 1977 considered this effect as the dominant one for the temperature delay).
3. The climate of Beit Harava is mostly affected by the Dead Sea breeze relative to the other stations around the Dead Sea, which opposed the penetration of the MSB. Thus, the relative cool wind coming from the Dead Sea during the morning being replaced by the hot wind of the MSB in the afternoon. This is less seen at Bet Haarava which is located 3 km away from the lake.

3.4 The pre-Mediterranean Sea breeze fronts

Pre-Mediterranean Sea breeze fronts (SBF) were first pointed-out over the southern Israel coast (Alpert and Rabinovich-Hadar, 2003). Gustiness graphs allowed us to witness that phenomenon at the Dead Sea as well. While the main SBF is noticed by the absolute peaks, the pre-sea breeze fronts become very clear in the secondary peaks of the gustiness (Fig 3). They can be seen in Sdom before 16:00 and after 16:00 in Hatzeva; a few tens of minutes before the SBF reaches the area.

Fig 7 shows the wind speed (left axis, red graph) and the gustiness (right axis, blue graph) in Sdom during the period of 9-12/08/2009. The two peaks in gustiness (G) can be easily noticed in each day. The higher G-peaks indicate the SBF of the MSB (with double-line arrows). These G peaks are followed by a rapid increase in wind speed that leads to the daily maximum around 18:00. The pre-SBF peaks have lower wind speeds and reach the area about 30 minute before the SBF peaks (marked by one-line arrows). Usually these G-peaks are followed by a small and temporary increase in the wind speed.

Fig 8 zooms-in on the pattern of one day from the last figure (Fig 7). It shows wind speed (V), gustiness (G) and specific humidity (SH) graphs on the 10/08/2009 in order to study the effect of the SBF and the pre-SBF on the humidity in stations around the Dead Sea. According to the gustiness graph, when the MSB reaches the area, the highest gustiness peak is reached at 17:20. In addition there are two pre-SBFs about one hour before the SBF. The wind speed gradually decreases from midday until a few minutes past 16:00, when the second pre-SBF arrives. In a few minutes the wind speed triples its intensity, and then weakens gradually until the SBF arrival at 17:20. At this time the wind speed climbs rapidly and reaches its daily peak. The specific humidity decreases also from midday and increases when the pre-SBF arrives. The most dominant increase in specific humidity (of about 30% and 25-50% in the relative humidity) appears when the SBF arrives. That means that the MSB brings higher humidity from the Mediterranean into the JRV. The increase in the humidity continues even after the post-SBF arrives.

It should be noticed that the pre-SBFs were not detected in all of the stations along the JRV. The reason is most likely the topography west of the stations as suggested next. For example, the topography to the northwest of the Beit Haarava station (steep and high cliffs) forces the breeze to fall suddenly from the mountains into the valley as it bursts through the barriers; hence, it does not allow for the penetration of the weaker pre-SBF. On the other hand, the cliffs are further away and lower to the northwest of Sdom and Hatzeva stations. There, the breeze penetrates more easily in to the valley; thus, the creation of the pre-SBF becomes possible.

4. Summary and Conclusions

The MSB is the most dominant wind in the JRV during the summer months (July-August). The fact that the MSB reaches the Dead Sea a few hours after it reaches the Sea of Galilee has been demonstrated. Our hypothesis is that the MSB reaches the stations along the JRV (from Kfar Blum to Hatzeva) according to their location from north to south. The distance from the Mediterranean Sea and the mountain height west to the station is dictating this well-defined chronological order. This was confirmed for the northern and central parts of the JRV. However, it becomes clear that the penetration of the breeze to the Dead Sea region is interrupted by its micro-climate. As a result, the breeze breaks into the southern parts of the Dead Sea and the evaporation ponds after it penetrates to its northern shores and after the Hazeva station in the Arava.

The MSB arrival to the JRV is investigated within the context of the surrounding complex topography. For example, it is well known that the wind gains high speed as a result of its descent from the mountains into the valley. But, here, a comparison between different parts of the JRV was performed. It was suggested that since there is a relatively small height difference between Kfar Blum to the mountains to the west, the wind speed of the MSB is about 50% weaker than its speed at the Kinneret and at the Dead Sea region. It was also shown that the wind reaches the highest velocity about two hours after it penetrates into the JRV, and then, it blows at high velocity for a few tens of minutes then calms down gradually.

The specific humidity rises with the MSB penetration time to the JRV. This signifies that the MSB is still humid after more than 100 km of blowing over land, and causes an increase in specific humidity while reaching the JRV.

Temperature reaches its peak in later afternoon hours in the southern JRV stations as compared to the north. A probable explanation for this is the JRV structure and distance from the Mediterranean coast. Since the JRV structure is the deepest and narrowest near Beit Haarava, the temperature peak is the latest in this station as compared to the other JRV stations.

Pre-SBF lines were detected about an hour before the breeze approached the stations in the southern DS evaporation ponds. The strong and brief associated with these secondary fronts have also a significant impact on the local climate, since they cause the rising of both specific and relative humidities in this arid region.

Acknowledgements

We wish to thank the Dead Sea Works for their generous grant, which enabled us to conduct our research. The German Helmholtz Association is gratefully acknowledged for funding this project within the Virtual Institute DESERVE (Dead Sea Research Venue) under contract number VH-VI-527.

References

Alpert, P., Cohen, A., Neumann, J. and Doron, E., 1982: ‘A model simulation of the summer circulation from the eastern Mediterranean past lake Kinneret in the Jordan valley’, Mon. Wea. Rev., **100**, 994–1006.

Alpert, P. and Eppel, A., 1985: ‘A proposed index for mesoscale activity’, J. Climate and App. Met., **24**, 472-480.

Alpert, P., Abramsky, R. and Neeman, B. U., 1990: 'The prevailing summer synoptic system in Israel - Subtropical High, not Persian Trough', Israel J. Earth Sci., **39**, 93-102.

Alpert, P. and Rabinovich-Hadar, M., 2003: ‘Pre- and post-sea-breeze frontal lines—A meso-γ-scale analysis over south Israel’, J. Atmos. Sci. **60,** 2994–3008.

Alpert, P. and Getenio, B., 1988: 'One-level diagnostic modelling of mesoscale surface winds in complex terrain. Part I: Comparison with three-dimentional modelling in Israel', Mon. Wea. Rev., **116,** 2025-2046.

Alpert, P., Shafir, H. and Issahary, D., 1997: ‘Recent changes in the climate at the Dead Sea — A preliminary study’, Clim. Change, **37**, 513– 537.

Ashbel, D., 1939: ‘The Influence of the Dead Sea on the Climate of Its Neighbourhood’, Quart. J. Roy. Met. Soc., **115**, 185–194.

Bitan, A., 1974: ‘The wind regime in the north-west section of the Dead-Sea’, Arch. Met. Geoph. Biokl., **22** (Ser B), 313–335.

Bitan, A., 1977: ‘The influence of the special shape of the Dead Sea and its environment on the local wind system’, Arch. Met. Geoph. Biokl., **24** (Ser B), 283–301.

Bitan, A., 1982: The Jordan Valley Project – A Case Study in Climate and Regional Planning, Energy and Buildings, **4**, 1-9.

Bitan, A. and Saaroni, H., 1992: ‘The horizontal and vertical extension of the Persian Gulf trough’, Int. J. Climatol., **12**, 733–747.

Cohen, S. and Stanhill, G., 1996: ‘Contemporary climate change in the Jordan Valley’, J. Appl. Meteor., **35**, 1051-1958.

Crosman, E. T. and Horel, J. D., 2010: 'Sea and lake breezes: A review of numerical studies', Bound.-Lay. Meteorol., **137**, 1-29.

Doron, E, Newmann, J., 1977: 'Land and mountain breezes with special attention to Israel Mediterranean coastal plain' Isr. Meteorol. Res. Pap. **1**, 109–122.

Feliks, Y., 2004: 'Nonlinear Dynamics and Chaos in the Sea and Land Breeze', Journal of the atmospheric sciences, **_61_(17)**.

Goldreich, Y., Druyan, L. M. and Berger, H., 1986: 'The interaction of valley/mountain winds with a diurnally veering sea/land breeze', J Climatol., **6**, 551–561.

Lensky, I. M. and Dayan, U., 2012: 'Continuous detection and characterization of the Sea Breeze in clear sky conditions using Meteosat Second Generation', Atmospheric Chemistry and Physics, **12**, 6505–6513.

Mahrer, Y., 1985: 'A numerical study of the effects of sea surface temperature on the sea land breeze circulation', Isr. J. Earth Sci., **34**, 91–95.

Saaroni, H. and Ziv, B., 2000: ‘Summer rainfall in a Mediterranean climate — the case of Israel: climatological–dynamical analysis’, Int. J. Climatol., **20**, 191–209.

Saaroni, H., Maza, E, and Ziv, B., 2004: ‘Summer sea breeze under suppressive synoptic forcing, in a hyper-arid city: Eilat, Israel’, Clim. Res., **26**, 213-220.

Segal, M., Mahrer, Y. and Pielke, R. A., 1983: 'A study of meteorological patterns associated with a lake confined by mountains - the Dead Sea case', Quart. J. R. Met. Soc., **109**, 549-564.

Segal, M., Mahrer, Y., Pielke, R. A. and Kessler, R. C., 1985: 'Model simulation of the summer daytime induced flows over southern Israel', Isr. J. Earth Sci., **34**, 39–46.

Shafir, H. and Alpert, P., 2011: ‘Regional and local climatic effects on the Dead-Sea evaporation’, Clim. Change**, 105**, 455-468.

Simpson, J. E., 1994: 'Sea breeze and local winds', Cambridge University Press, 234pp., 1994.

Skibin, D. and Hod, A., 1979: 'Subjective analysis of mesoscale flow patterns in Northern Israel', J. Appl. Meteorol., **18**, 329-338.

Figures Captions

Fig. 1. Geographic location of the Jordan Rift Valley and the location of the meteorological stations used in this study from North to South: Kfar Blum (1), Beit Tzaida (2), Gilgal (3), Beit Haarava (4), Sdom (5) and Hatzeva (6).

Fig. 2. Mean daily wind speed in JRV stations in July-August during 2008-2009. The legend presents the stations from north to south. The arrows point to the peak for each station. Time span of SB arrival to the JRV goes all the way from 14:00 (station 1) to 19:20 (station 5).

Fig. 3. As in Fig. 2 but for the gustiness.

Fig. 4. As in Fig.2 but for the 10 min difference in the wind speed. The difference is defined as the subtraction of each 10 min data from the measurements which were taken 20 min before.

Fig. 5. As in Fig. 2 but for the specific humidity. The arrows indicate the time when the specific humidity starts to increase.

Fig. 6. As in Fig. 2 but for temperature.

Fig. 7. Wind speed (V red) and gustiness (G blue) in Sdom during 9-12/08/2009. Double-line arrows point at the SBF while one-line arrows point at the pre SBF. The V scale in ms^{-1} is on the left while that of G scale is on the right.

Fig. 8. Zoom in on the Wind speed (red), gustiness (blue) and specific humidity (green) in Sdom at 10/08/2009. Wind speed and specific humidity are on the left axis, gustiness is on the right axis. Double-line arrow points at the SBF and one-line arrows point at the pre SBF.

Table Caption

Tab. 1. Topographical characteristics of the measuring stations

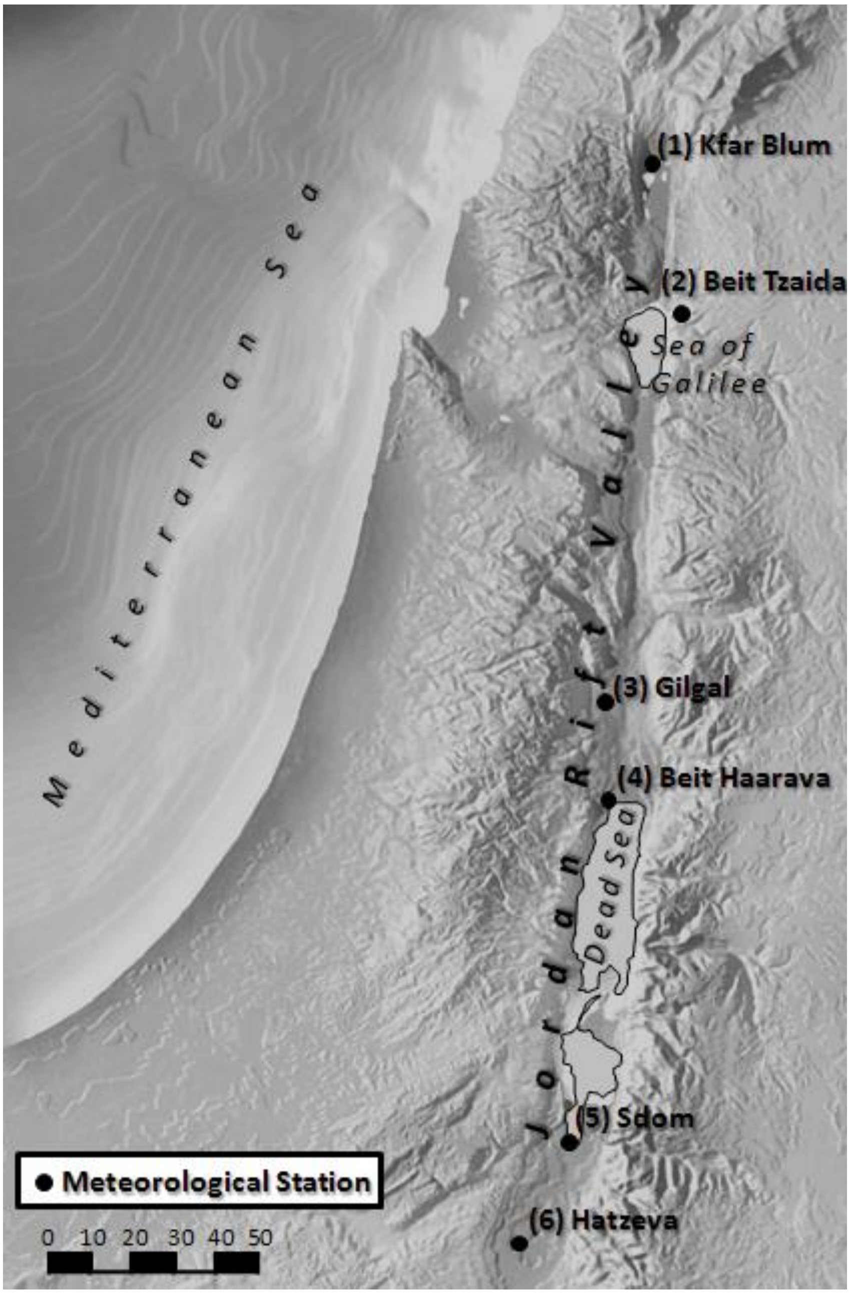

Fig. 1*: Geographic location of the Jordan Rift Valley and the location of the meteorological stations used in this study from North to South: Kfar Blum (1), Beit Tzaida (2), Gilgal (3), Beit Haarava (4), Sdom (5) and Hatzeva (6).*

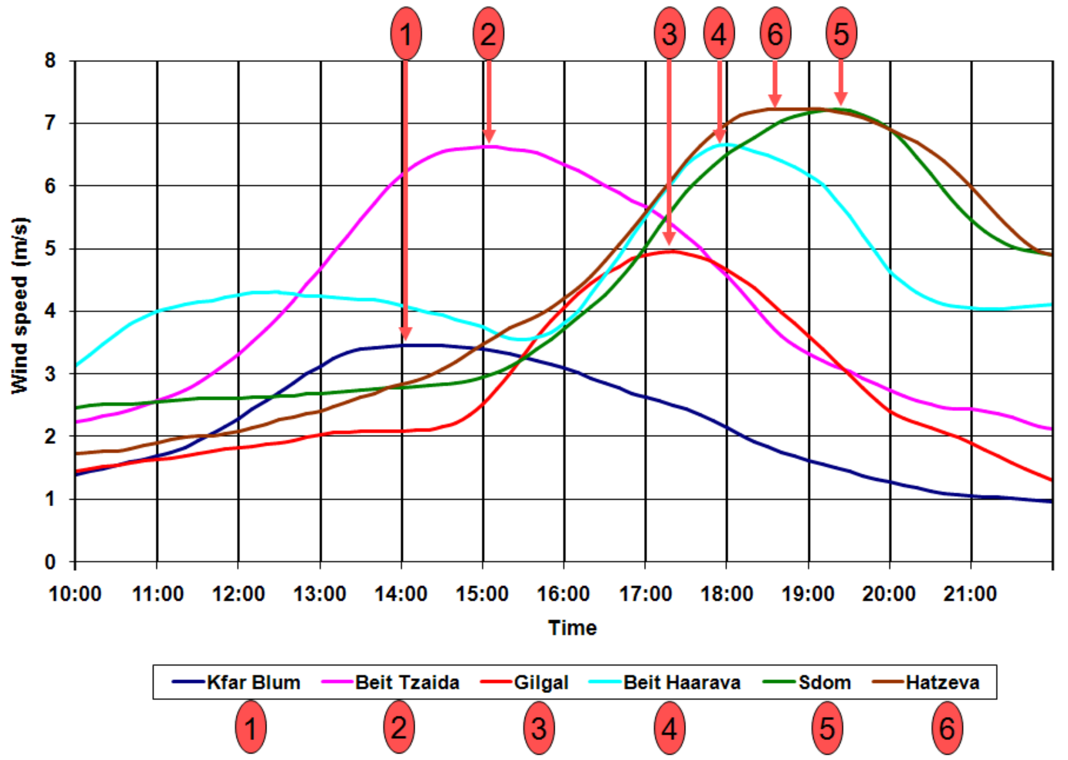

Fig. 2: *Mean daily wind speed in JRV stations in July-August during 2008-2009. The legend presents the stations from north to south. The arrows point to the peak for each station. Time span of SB arrival to the JRV goes all the way from 14:00 (station 1) to 19:20 (station 5).*

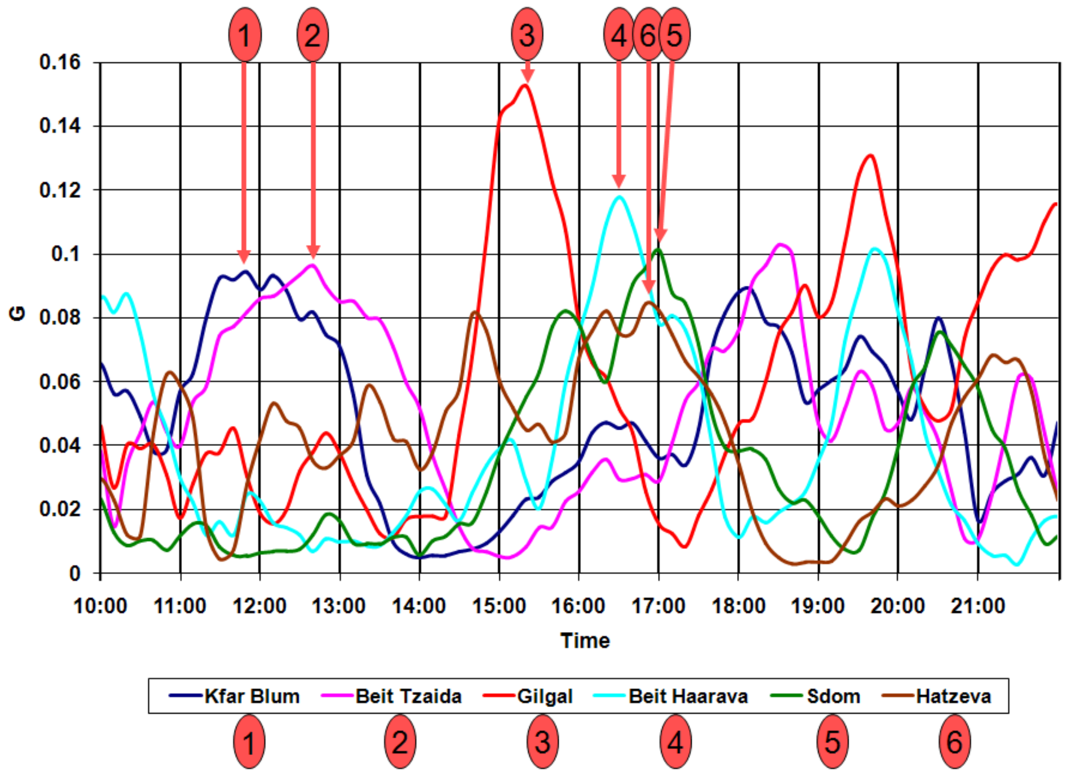

Fig. 3: *As in Fig. 2 but for the gustiness.*

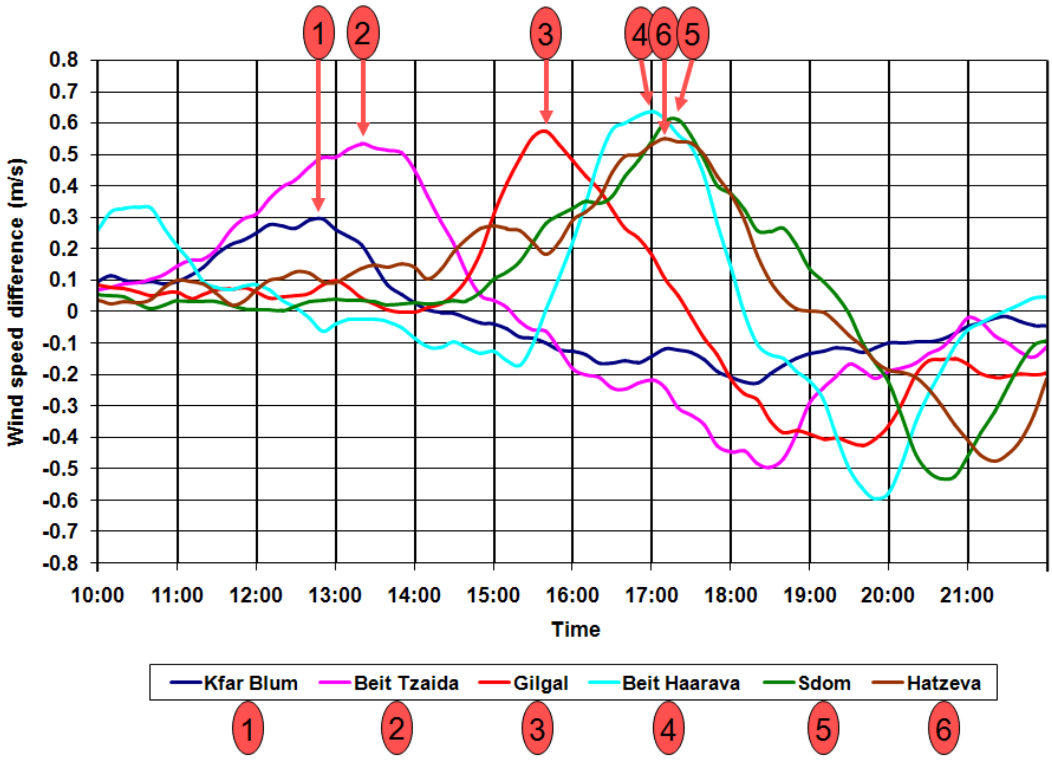

Fig. 4: *As in Fig.2 but for the 10 min difference in the wind speed. The difference is defined as the subtraction of each 10 min data from the measurements which were taken 20 min before.*

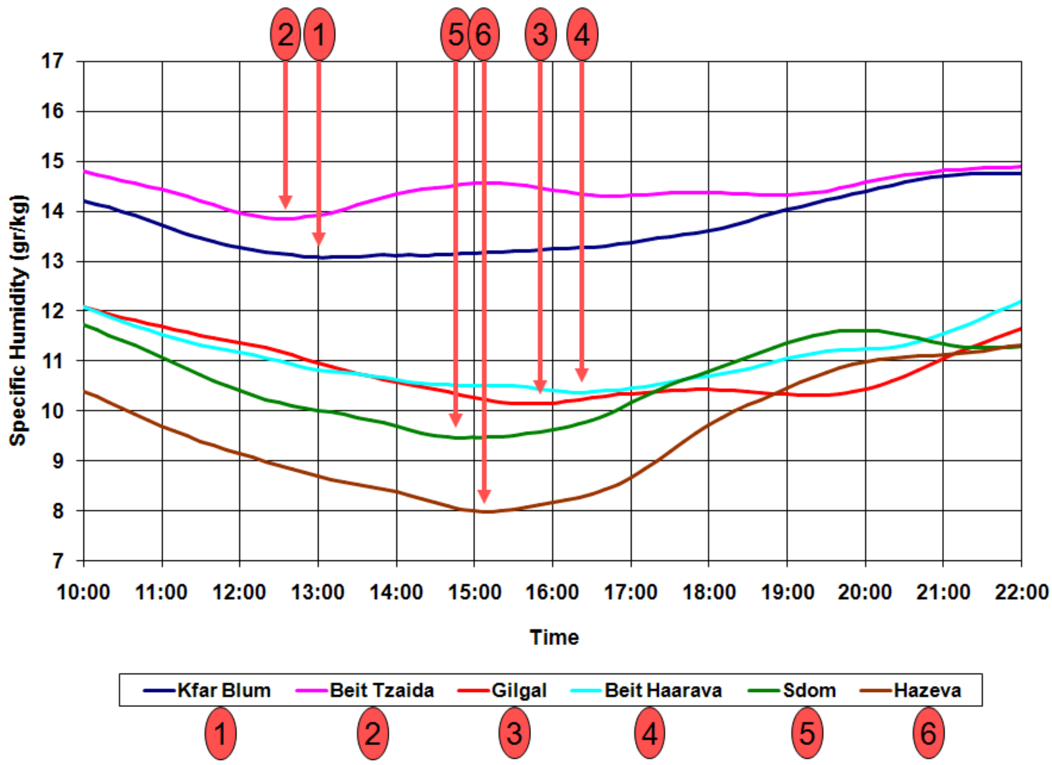

Fig. 5*: As in Fig. 2 but for the specific humidity. The Arrows indicate the time when the specific humidity starts to increase.*

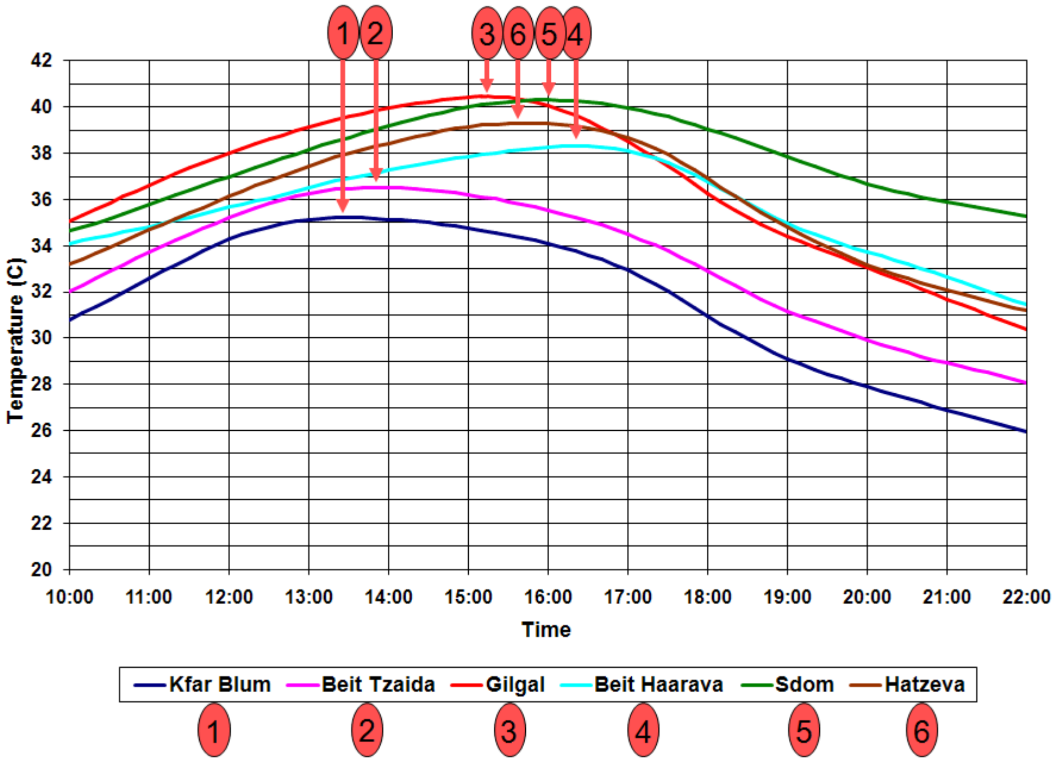

Fig. 6: *As in Fig. 2 but for temperature.*

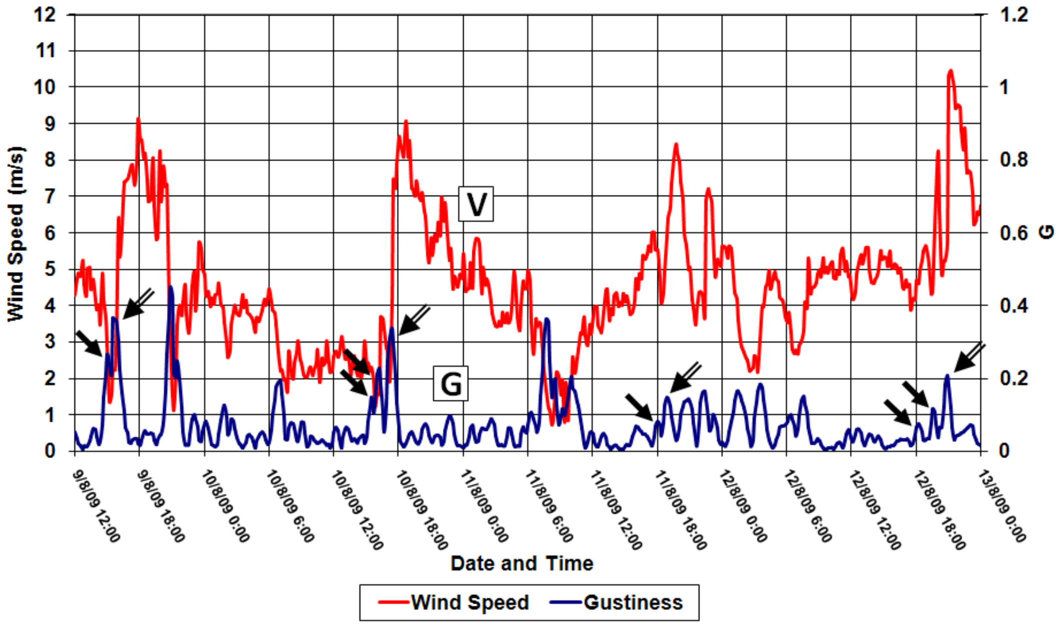

Fig.7: *Wind speed (V red) and gustiness (G blue) in Sdom during 9-12/08/2009. Double-line arrows point at the SBF while one-line arrows point at the pre SBF. The V scale in ms^{-1} is on the left while that of G scale is on the right.*

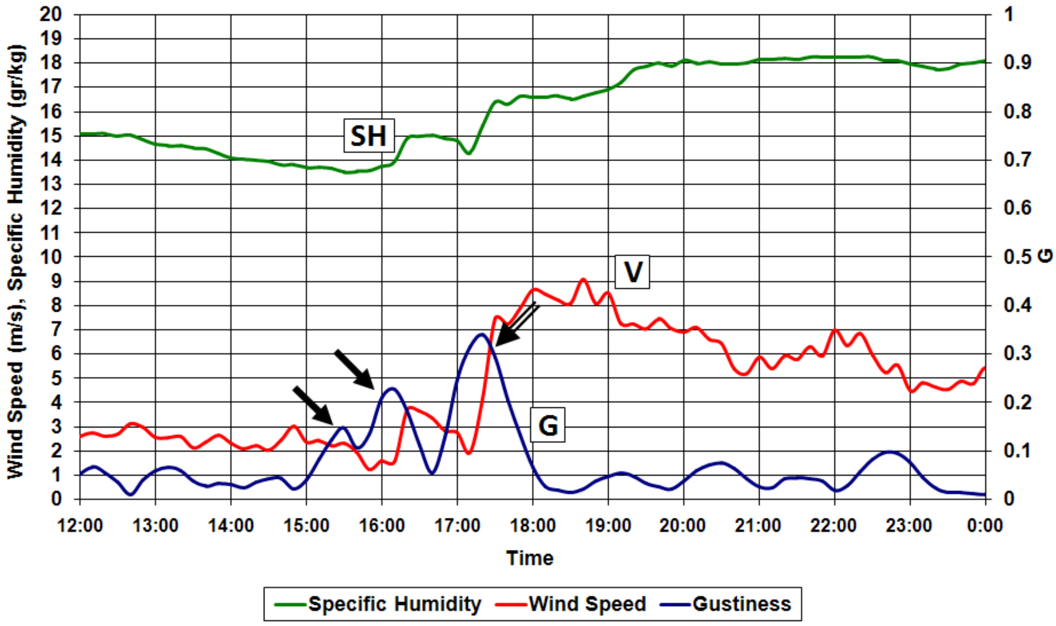

Fig. 8: Zoom in on the *Wind speed (red), gustiness (blue) and specific humidity (green) in Sdom at 10/08/2009. Wind speed and specific humidity are on the left axis, gustiness is on the right axis. Double-line arrow points at the SBF and one-line arrows point at the pre SBF.*

No.	Station	Longitude (deg)	Latitude (deg)	Elevation (m)	Distance from The Mediterranean Sea Shore (km)	Height of Mountain to The West Of Station (m)	Maximum Height Difference between Mountain to the West of the Station (m)
1	Kfar Blum	35.607948	33.172519	75	40	800	725
2	Beit Tzaida	35.633089	32.904106	-200	55	750	950
3	Gilgal	35.448221	32.000306	-255	65	900	1,155
4	Beit Haarava	35.497673	31.808429	-330	75	900	1,230
5	Sdom	35.397666	30.993227	-388	110	500	888
6	Hatzeva	35.246680	30.774858	-135	120	500	635

Tab. 1. Topographical characteristics of the measuring stations